nature reviews earth & environment

https://doi.org/10.1038/s43017-024-00624-z

Supplementary information

Hydroclimate volatility on a warming Earth

In the format provided by
the authors and unedited

Hydroclimate volatility on a warming Earth

Daniel L. Swain[1,2,3†], Andreas F. Prein[3,4], John T. Abatzoglou[5], Christine M. Albano[6], Manuela Brunner[7,8,9], Noah S. Diffenbaugh[10], Deepti Singh[11], Christopher B. Skinner[12] & Danielle Touma[13]

[1] University of California Agriculture and Natural Resources, Davis, CA, USA

[2] Institute of the Environment and Sustainability, University of California, Los Angeles, Los Angeles, CA, USA

[3] Capacity Center for Climate and Weather Extremes, National Center for Atmospheric Research (NCAR), Boulder, CO, USA

[4] Institute for Atmospheric and Climate Science, ETH Zürich, Zurich, Switzerland

[5] Management of Complex Systems, University of California, Merced, Merced, CA, USA

[6] Division of Hydrologic Sciences, Desert Research Institute, Reno, NV, USA

[7] Department of Environmental Systems Science, ETH Zürich, Zurich, Switzerland

[8] WSL Institute for Snow and Avalanche Research SLF, Davos, Switzerland

[9] Climate Change, Extremes and Natural Hazards in Alpine Regions Research Center CERC, Davos, Switzerland

[10] Doerr School of Sustainability, Stanford University, Stanford, CA, USA

[11]School of the Environment, Washington State University, Vancouver, WA, USA

[12] Department of Environmental Earth and Atmospheric Sciences, University of Massachusetts, Lowell, Lowell, MA, USA

[13] Institute for Geophysics, University of Texas, Austin, Austin, TX, USA

[†]**e-mail:** dlswain@ucanr.edu

Summary of supplementary information contents

This supplementary information document contains:

1) A complete description of the methods used to calculate the "hydroclimate volatility" metric defined for the first time and used in this review in the "Supplementary Methods" section.

2) Supplementary discussion describing the illustrative historical hydroclimate whiplash events quantified in Figure 1 in the main manuscript in the "Supplementary Discussion" section.

3) Figures intended to augment the key findings depicted in the figures contained in the main manuscript in the "Supplementary Figures" section.

Supplementary Methods

Here, we describe the methods used to calculate the "hydroclimate whiplash" metric that forms the basis of certain quantitative claims in the text as well as Figures 2 and 3. We use atmospheric reanalysis data from two separate sources (ERA-5[1] and NOAA-CIRES-DOE 20CRv3 (henceforth and in the main manuscript "NCD20C"))[2] to address the potential biases present in any single reanalysis, and the SSP3-7.0 scenario in a single model large climate model ensemble[3] (CESM2-LENS) to calculate monthly-scale Standardized Precipitation Evapotranspiration Index values (SPEI, using the Penman-Monteith approach for calculating potential evapotranspiration[4]). Using these monthly SPEI values, we define a "hydroclimate whiplash event" as one which occurs when the temporal difference in SPEI (positive or negative) meets or exceeds the value associated with an approximate 10-year recurrence interval in a single reanalysis or climate model grid box within the reference period (1940-1980). The underlying SPEI calculation is at grid box level and relative to the underlying seasonal cycle during the historical SPEI calibration period, and thus accounts for the local background degree of hydroclimate variability and seasonality.

We do so on two separate timescales: sub-seasonal and interannual. To calculate the magnitude of sub-seasonal SPEI transitions used in determining whiplash, we derive differences between SPEI3 (i.e., the 3-month moving average of monthly SPEI) over a moving window itself up to three months long. For a given June-August period, for example, we calculate three differences in SPEI3: August SPEI3 minus July SPEI3, August SPEI3 minus June SPEI3, and August SPEI3 minus May SPEI3. From these, we calculate either the maximum value (if the sign of the difference is positive, corresponding to dry to wet transitions) or the minimum value (if the sign of the difference is negative, corresponding to wet to dry transitions) and store it for each location in each month. To establish a historical baseline for local whiplash occurrence, the subsequent location-specific time series are used to calculate the 99.4th/0.6th percentile threshold in the 1940-1980 period (i.e., resulting in one exceedance each for wet-to-dry and dry-to-wet transitions per

decade). To calculate interannual whiplash, we repeat the same process using SPEI12 (i.e., the 12-month moving average of monthly SPEI). A whiplash event is defined to have occurred if the stored SPEI temporal difference on the relevant time scale exceeds the local baseline threshold. To quantify the total number of hydroclimate whiplash events in a given location as well as temporal trends, we sum the combined counts of wet-to-dry and dry-to-wet whiplash events to derive a composite whiplash metric resulting in an combined event frequency of approximately once per five years during the baseline period.

In Figures 2 and 3 in the main manuscript, in the supplementary figures below, and as discussed elsewhere in the main text, global hydroclimate whiplash changes are reported both as global mean values and also separated into "land" (defined as all grid boxes that are neither ocean nor inland water (e.g., lakes)) or "ocean" (defined all grid points classified as either ocean or inland water (e.g., lakes).

For the purposes of this review, we group various anthropogenic emissions trajectories used to conduct and assess coordinated climate model simulations[5] into two broad categories: "high emissions" trajectories (including RCP8.5, SSP5-8.5 and SSP3-7.0) and "moderate emissions" trajectories (including RCP6.0, RCP4.5, and SSP2-4.5), though we note that the SSP scenarios used in the CMIP6 experiments incorporate more socioeconomic factors than do the RCP scenarios used in CMIP5. The level of global warming associated with high emissions trajectories might be experienced under either continued acceleration of anthropogenic greenhouse gas emissions (which observed emission trends as of 2023 do not support[6]) or if the overall climate sensitivity is considerably higher than median estimates[7]. The level of warming associated with moderate emissions trajectories is compatible with observed stabilization of emission trends[8] and is within range of plausible climate policy outcomes as of 2023[7]. In cases lower emission trajectories are considered, the specific warming level is noted (for example, 2°C). Higher emission scenarios (such as RCP8.5 and SSP3-7.0, which yield warming well in excess of 3°C by 2100) can still be used to estimate climate impacts at lower levels of warming (for example, 2°C) that are consistent with lower emission scenarios[3].

Supplementary Discussion

The following brief summaries describe the illustrative hydroclimate whiplash events highlighted in Figure 1 in the main manuscript.

North-Central U.S.

Change in SPEI-12: January 2020 - January 2021

Maximum Change in SPEI-12: -5.7

Extreme precipitation beginning in the spring of 2019, combined with antecedent wet soils, led to record flooding across the Northern U.S. Plains and Upper Midwest. Water levels reached record peaks at approximately 75 locations across the Missouri River Basin, and much of the river and its tributaries remained above flood stage for most of the year. Extreme rain and flooding led to planting delays, a shortening of the growing season, and nearly 20 million acres of unplanted agricultural land[9]. Total estimated losses to agriculture, residential and commercial property, and public infrastructure from flooding across the region was $13.4 billion[10].

Less than one percent of the region was in drought at the start of 2020. Drought conditions developed across the region in the spring and spread throughout the Northern U.S. Plains by fall. By the end of November, portions of eastern Wyoming, eastern Montana, North Dakota and South Dakota were in a state of extreme drought (D3 classification U.S. Drought Monitor). A lack of rainfall led to impacts on fall season seeding and food supplies for livestock. A lack of snow, dry grasses, and a high-wind event led to several grass fires across the region in January 2021. Drought intensified throughout an abnormally hot 2021, reducing hydropower production and livestock herd numbers, and facilitating wildfire activity across 6.5 million acres[11].

Pacific Southwest

Change in SPEI-12: October 2022 - October 2023

Maximum Change in SPEI-12: 5.5

2022 marked the third consecutive year of widespread drought across California and the Great Basin. California experienced its driest ever January – October period[12], ending the 2022 water year (October 1 2021 – September, 30 2022) with state reservoir storage at 69% of average[13]. Wildfires associated with dry conditions in the state burned over 362,000 acres and destroyed 772 structures[14]. The 2023 water year (October 1 2022 – September 30 2023) brought record precipitation, snowpack, and flooding to California and Nevada. California (Nevada) experienced its 7th (3rd) wettest December-March since records began in 1895. Winter storms and the associated flooding, rockslides, and fallen trees, contributed to at least 22 deaths. Levees broke across California, inundating homes and agricultural land with water, forcing widespread evacuations[15].

Northern and Central Europe

Change in SPEI-12: January 2018 - January 2019

Maximum Change in SPEI-12: -6.2

2017 was an anomalously wet year across Northern and Central Europe, with particularly heavy rainfall during the summer and fall seasons. Extreme precipitation caused widespread flooding across Germany that inundated streets and underground rail stations and led to transport delays[16]. In 2018, a dry and exceptionally warm spring season initiated drought across much of Northern and Central Europe. Hot and dry conditions continued throughout the summer leading to the combined hottest and driest growing season on record. Widespread crop losses resulted in farmer compensation of €340 million in Germany and €116 million in Sweden[17]. Depleted water reserves led to ecosystem damage, reduced energy production, and issues with drinking water[18].

Central America

Change in SPEI-12: November 2019 - November 2020

Maximum Change in SPEI-12: 5.6

2019 was the fifth consecutive year of drought across Central America. Impacts on agricultural production were particularly acute in the Central American Dry Corridor countries of Guatemala, El Salvador, Honduras and Nicaragua where an estimated 2.2 million people suffered crop losses[19]. In 2020, Central America was hit by two strong tropical cyclones, Hurricane Eta and Hurricane Iota. Widespread flooding and landslides across mountainous terrain killed 200 people and displaced more than 500,000 across the region[20].

Southern Chile and Argentina

Change in SPEI-12: December 2016 - December 2017

Maximum Change in SPEI-12: 5.6

Southern Chile and Argentina experienced anomalously dry conditions during the majority of 2016. In western Patagonia, precipitation deficits of at least 50% led to decreased streamflow, anomalously high

wildfire activity and vegetation die-off[21]. In 2017, anomalously wet conditions across Central and Southern Chile were punctuated by several extreme rainfall events, including a December storm that led to a catastrophic landslide in Villa Santa Lucía, Chile, destroying half of the village and killing 22 people[22].

Southeast Australia

Change in SPEI-12: December 2019 - December 2020

Maximum Change in SPEI-12: 4.6

2019 was the third consecutive year of drought in Southeast Australia. Production of wheat, barley, and rice dropped by 63%, 43% and 90% respectively. The dry land surface amplified heat wave temperatures by up to 2.5°C and led to extensive wildfires that burned over 5.8 million hectares during early 2020[23]. Wetter conditions prevailed throughout Southeast Australia in 2020, with heavy rain and major flooding during February (more than 300% of the average monthly total during a 4-day span)[24] and record setting daily rainfall totals and flash flooding in December[25].

Iran, Pakistan, and Eastern Arabian Peninsula

Change in SPEI-3: May 2022 – August 2022

Maximum Change in SPEI-3: 12.8

Dry conditions prevailed across Iran, Pakistan, and the Eastern Arabian Peninsula during spring and early summer. In Pakistan, for example, a lack of precipitation and a spring heat wave brought mild to severe drought across western portions of the country prompting the government to advise farmers to take preemptive measures. The summer months brought record precipitation to the region. In Pakistan, monsoon rains drove extreme flooding, killing at least 900 people and leaving 30 million homeless[26]. Iran experienced catastrophic flooding and landslides that killed at least 69 people, damaged more than 20,000 homes, and shut down airports and highways[27].

Southern China

Change in SPEI-3: June 2022 – September 2022

Maximum Change in SPEI-3: -6.6

In 2022, Southern China experienced its wettest spring since 1961. Floods and landslides killed at least 32 people, damaged crops and homes, and resulted in over $600 million in economic losses[28]. During summer, persistent heat waves combined with a lack of precipitation drove widespread drought. Low water levels affected hydropower production both locally and in downstream locations that import much of their energy from the drought affected areas[29].

West Africa

Change in SPEI-3: June 2020 – September 2020

Maximum Change in SPEI-3: 5.8

Hot and dry conditions prevailed across much of the West African Sahel during the late spring and early summer of 2020[30]. Beginning in July, conditions became anomalously wet, and several extreme rainfall events brought flooding to the region. The floods led to outbreaks of vector-borne diseases, including Rift Valley fever and Chikungunya, as well as the displacement of over 225,000 people in Niger, and an estimated $13 million in crop losses in Nigeria[31].

East Africa

Change in SPEI-3: September 2023 – December 2023

Maximum Change in SPEI-3: 6.4

A prolonged drought impacted the eastern Horn of Africa between 2020 and 2023, causing widespread crop and livestock loss, conflict, and food insecurity for over 20 million people[32]. The subsequent 2023 July-September dry season was anomalously hot and dry across much of the region, further reducing water resources and crop yields. Extreme rain and flooding in Kenya, Ethiopia, and Somalia during the 2023 fall harvest season destroyed crops, forced 2 million people to evacuate their homes, and left 4 million people without food and income[33].

Supplementary Figures

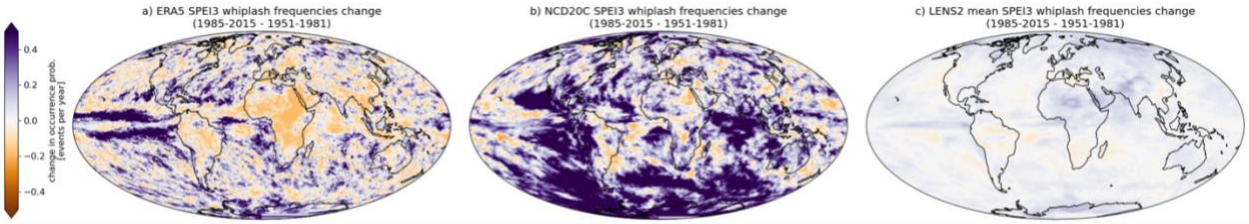

Supplementary Fig. 1. Historical changes in hydroclimate whiplash frequency, ERA5 and NCD20C versus LENS2. a,b | Global map of historical (1985-2015 minus 1951-1981) differences in sub-seasonal (defined as 3-month SPEI with large transitions within 3 months) hydroclimate whiplash frequency in the ERA5 (a) and NCD20C (b) reanalysis. **b** | Same as a, but for the CESM-LENS2 climate model large ensemble mean.

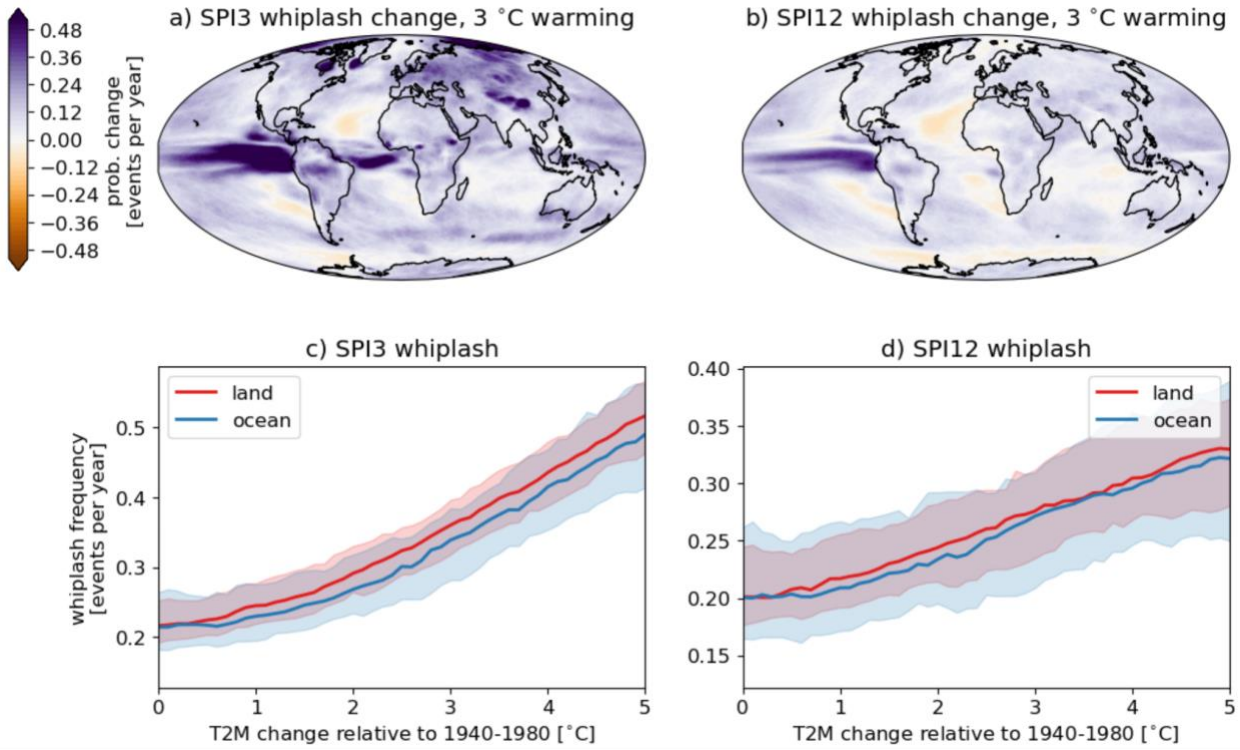

Supplementary Fig. 2. Projected hydroclimate whiplash trends using a precipitation-only metric (SPI) in a warming climate. **a** | Global map of projected sub-seasonal (up to 3 month) hydroclimate whiplash in the CESM-LENS2 climate model large ensemble at 3°C of global mean warming. **b** | Same as a, but for inter-annual (up to 12 month) whiplash. **c** | Trends in sub-seasonal (up to 3 month) hydroclimate whiplash in the CESM-LENS2 climate model large ensemble as a function of projected global mean warming. **d** | Same as c, but for inter-annual (up to 12 month) whiplash. In map plots, purple colors represent increases in whiplash frequency and orange colors decreases in whiplash frequency (both in units of events per decade). The light red and blue shaded regions represent the 5th to 95th percentile ensemble spread for the CESM-LENS2 whiplash counts. In the CESM2-LENS simulations, hydroclimate whiplash increases strongly with warming over nearly all global land areas and most global ocean areas outside of the subtropics, and the rate of sub-seasonal whiplash increase accelerates particularly over land between 1°C and 3°C of global mean warming. All global mean temperature values are calculated relative to the 1940-1980 reference period. This figure, which depicts changes in projected whiplash using a precipitation-only metric (the Standardized Precipitation Index, or SPI) is intended to complement Figure 3 (identical except that it depicts changes in whiplash using a metric encompassing both precipitation and evaporative demand, i.e., the Standardized Precipitation-Evaporation Index, or SPEI).

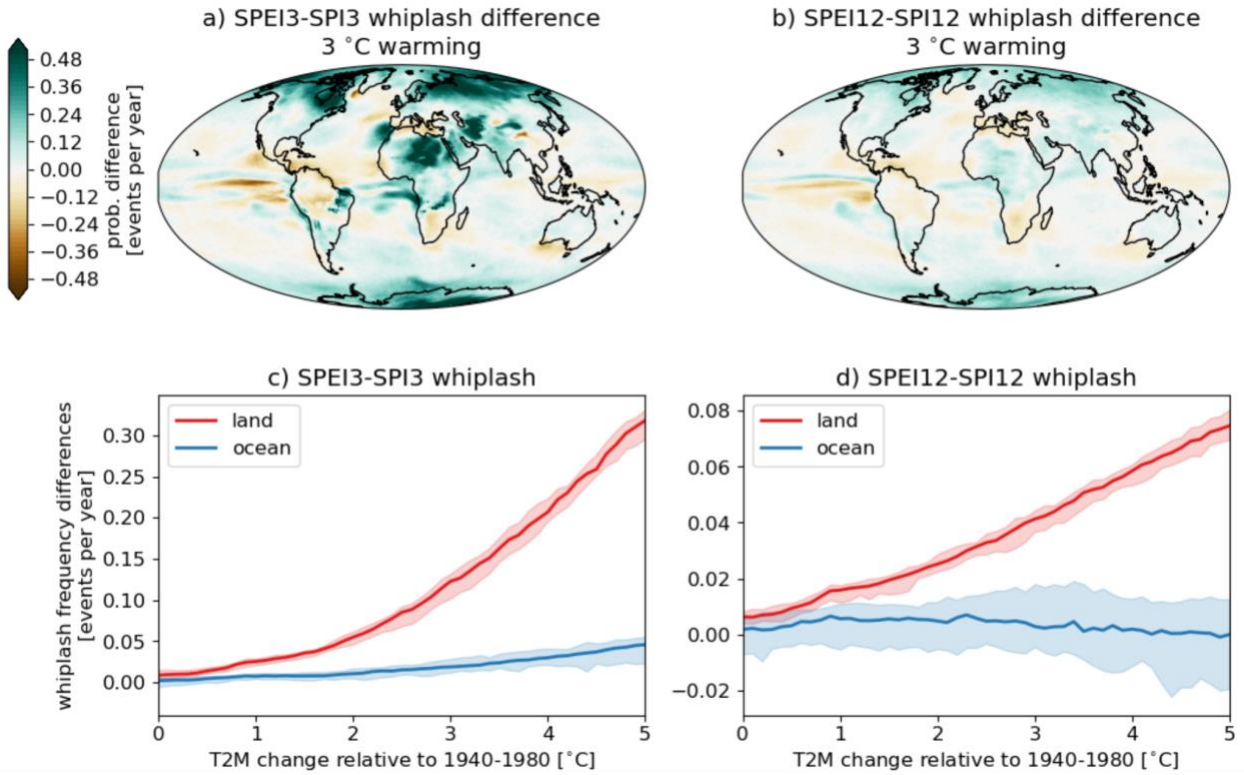

Supplementary Fig. 3. Difference in projected hydroclimate whiplash trends in a warming climate, SPEI vs. SPI. **a** | Global map of difference in projected sub-seasonal (up to 3 month) hydroclimate whiplash change in the CESM-LENS2 climate model large ensemble at 3°C of global mean warming using SPEI versus SPI-based metrics. **b** | Same as a, but for inter-annual (up to 12 month) whiplash. **C.** Difference in trends in sub-seasonal (up to 3 month) hydroclimate whiplash in the CESM-LENS2 climate model large ensemble as a function of projected global mean warming using SPEI versus SPI-based metrics. **d** | Same as c, but for inter-annual (up to 12 month) whiplash. In map plots, green colors represent locations where increases in whiplash frequency are larger using the SPEI-based metric, and brown colors represent locations where increases in whiplash frequency are larger using the SPI-based metric (both in units of events per decade). The light red and blue shaded regions in panels c) and d) represent the 5th to 95th percentile ensemble spread for the difference in CESM-LENS2 whiplash counts for SPEI vs SPI-based metrics. All global mean temperature values are calculated relative to the 1940-1980 reference period.

Supplementary References

1 Hersbach, H. *et al.* The ERA5 global reanalysis. *Quarterly Journal of the Royal Meteorological Society* **146**, 1999-2049, doi:https://doi.org/10.1002/qj.3803 (2020).

2 Slivinski, L. C. *et al.* Towards a more reliable historical reanalysis: Improvements for version 3 of the Twentieth Century Reanalysis system. *Quarterly Journal of the Royal Meteorological Society* **145**, 2876-2908, doi:https://doi.org/10.1002/qj.3598 (2019).

3 Rodgers, K. B. *et al.* Ubiquity of human-induced changes in climate variability. *Earth Syst. Dynam.* **12**, 1393-1411, doi:10.5194/esd-12-1393-2021 (2021).

4 Vicente-Serrano, S. M., Beguería, S. & López-Moreno, J. I. A Multiscalar Drought Index Sensitive to Global Warming: The Standardized Precipitation Evapotranspiration Index. *Journal of Climate* **23**, 1696-1718, doi:https://doi.org/10.1175/2009JCLI2909.1 (2010).

5 Eyring, V. *et al.* Overview of the Coupled Model Intercomparison Project Phase 6 (CMIP6) experimental design and organization. *Geosci. Model Dev.* **9**, 1937-1958, doi:10.5194/gmd-9-1937-2016 (2016).

6 Hausfather, Z. & Peters, G. Emissions – the 'business as usual' story is misleading. *Nature* **577**, 618-620, doi:10.1038/d41586-020-00177-3 (2020).

7 Marvel, K. *et al.* in *Fifth National Climate Assessment* (eds A. R. Crimmins *et al.*) Ch. 2, (U.S. Global Change Research Program, 2023).

8 Gidden, M. J. *et al.* Global emissions pathways under different socioeconomic scenarios for use in CMIP6: a dataset of harmonized emissions trajectories through the end of the century. *Geosci. Model Dev.* **12**, 1443-1475, doi:10.5194/gmd-12-1443-2019 (2019).

9 Umphlett, N. *The Historic Year of 2019*, <https://hprcc.unl.edu/pdf/2019Extremes.pdf> (2020).

10 National-Centers-for-Environmental-Information. *U.S. Billion-Dollar Weather and Climate Disasters*, <https://www.ncei.noaa.gov/access/billions/events/US/2019?disasters[]=all-disasters> (2024).

11 Umphlett, N. A., M. Woloszyn, B.A. Parker, F.A. Akyuz, A.R. Bergantino, S. Brotherson, D. Crow Ghost, M., Downey, L. Edwards, T. Hadwen, Z. Hoylman, K. Jencso, W. Kelley, A. Klein, D. Kluck, D. Longknife, K. Low, R., Mahmood, M. Meehan, G. Rush, C.J. Stiles, and S. Tangen. *DROUGHT IN THE U.S.: NORTHERN PLAINS AND CANADIAN PRAIRIES*, <https://www.drought.gov/sites/default/files/2023-04/2020-2021-Drought-US-Northern-Plains-and-Canadian-Prairies.pdf> (2022).

12 National-Centers-For-Environmental-Information. *Regional Drought Overview, West Overview*, <https://www.ncei.noaa.gov/access/monitoring/monthly-report/drought/202213#:~:text=As%202022%20ended%2C%20the%20epicenter,Basin%20and%20north%20central%20Montana.&text=Based%20on%20the%20Palmer%20Drought%20Inde

x%2C%202022%20began%20with%2059.4,experiencing%20moderate%20to%20extreme%20drought.> (2022).

13 California-Department-of-Water-Resources. *New Water Year Begins Amid Preparations for Continued Drought*, <https://water.ca.gov/News/News-Releases/2022/Oct-22/New-Water-Year-Begins-Amid-Preparations-for-Continued-Drought> (2022).

14 Cart, J. *By the numbers: California's mild 2022 wildfire season*, <https://calmatters.org/environment/wildfires/2022/12/california-wildfires-2022/> (2022).

15 California-Nevada-River-Forecast-Center. *Heavy Precipitation Events, California and Nevada*, <https://www.cnrfc.noaa.gov/storm_summaries/dec2022Jan2023storms.php> (2023).

16 Reuters. *Europe storms: at least six dead as winds and flooding create chaos*, <https://www.theguardian.com/weather/2017/oct/30/europe-storms-at-least-six-dead-as-winds-and-flooding-create-chaos> (2017).

17 Bastos, A. *et al.* Direct and seasonal legacy effects of the 2018 heat wave and drought on European ecosystem productivity. *Science Advances* **6**, eaba2724, doi:10.1126/sciadv.aba2724 (2020).

18 Brakkee, E., van Huijgevoort, M. H. J. & Bartholomeus, R. P. Improved understanding of regional groundwater drought development through time series modelling: the 2018–2019 drought in the Netherlands. *Hydrol. Earth Syst. Sci.* **26**, 551-569, doi:10.5194/hess-26-551-2022 (2022).

19 World-Food-Programme. *Erratic weather patterns in the Central American Dry Corridor leave 1.4 million people in urgent need of food assistance*, <https://www.wfp.org/news/erratic-weather-patterns-central-american-dry-corridor-leave-14-million-people-urgent-need> (2019).

20 Sarah Marsh, S. M. *Storms that slammed Central America in 2020 just a preview, climate change experts say*, <https://www.reuters.com/article/idUSKBN28D2V4/> (2020).

21 Garreaud, R. D. Record-breaking climate anomalies lead to severe drought and environmental disruption in western Patagonia in 2016. *Climate Research* **74**, 217-229 (2018).

22 Somos-Valenzuela, M. A., Oyarzún-Ulloa, J. E., Fustos-Toribio, I. J., Garrido-Urzua, N. & Chen, N. The mudflow disaster at Villa Santa Lucía in Chilean Patagonia: understandings and insights derived from numerical simulation and postevent field surveys. *Nat. Hazards Earth Syst. Sci.* **20**, 2319-2333, doi:10.5194/nhess-20-2319-2020 (2020).

23 Devanand, A. *et al.* Australia's Tinderbox Drought: An extreme natural event likely worsened by human-caused climate change. *Science Advances* **10**, eadj3460, doi:10.1126/sciadv.adj3460.

24 Australian-Institute-For-Disaster-Resilience. *Major Incidents Reports 2019-20*, <https://knowledge.aidr.org.au/media/8049/aidr_major-incidents-report_2019-20.pdf> (2019).

25 Australian-Associated-Press. *Man killed in Queensland flood waters as wild weather leaves NSW reeling*, <https://www.theguardian.com/australia-news/2020/dec/17/heavy-rain-and-storms-leave-much-of-nsw-reeling-as-wild-weather-brings-chaos> (2020).

26 Hong, C.-C. *et al.* Causes of 2022 Pakistan flooding and its linkage with China and Europe heatwaves. *npj Climate and Atmospheric Science* **6**, 163, doi:10.1038/s41612-023-00492-2 (2023).

27 Ramin Mostaghim, S. M., Mohammed Tawfeeq, Mostafa Salem, and Ivana Kottasová. *Iran flash flooding and mudslides leave at least 69 people dead*, <https://www.cnn.com/2022/07/31/middleeast/iran-floods-mudslides-weather-climate-intl/index.html> (2022).

28 Gan, N. *Torrential rains kill dozens in southern China as climate change amplifies flood seasons*, <https://www.cnn.com/2022/06/09/china/southern-china-flooding-climate-change-rains-intl-hnk/index.html> (2022).

29 Yang, M. *Extreme Weather Is Brutalizing Asia*, <https://foreignpolicy.com/2022/08/24/extreme-weather-asia-climate-change-floods-droughts-heatwave/> (2022).

30 Reliefweb. *West Africa Seasonal Monitor (01-10 June 2020)*, <https://reliefweb.int/report/mali/west-africa-seasonal-monitor-01-10-june-2020> (2020).

31 Thomas, N. P., Anyamba, A., Tubbs, H. & Bishnoi, B. Evaluation of Extreme Soil Moisture Conditions During the 2020 Sahel Floods and Implications for Disease Outbreaks. *Geophysical Research Letters* **49**, e2022GL099872, doi:https://doi.org/10.1029/2022GL099872 (2022).

32 Paddison, L. *Catastrophic drought that's pushed millions into crisis made 100 times more likely by climate change, analysis finds*, <https://www.cnn.com/2023/04/27/africa/drought-horn-of-africa-climate-change-intl/index.html> (2023).

33 Oxfam. *East Africa's floods decimate almost entire season harvest and leave over four million people with no food or income.*, <https://www.oxfam.org/en/press-releases/east-africas-floods-decimate-almost-entire-season-harvest-and-leave-over-four> (2023).